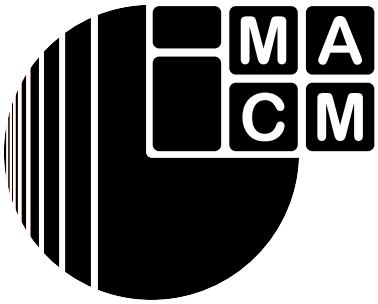

Bergische Universität Wuppertal

Fachbereich Mathematik und Naturwissenschaften

Institute of Mathematical Modelling, Analysis and Computational Mathematics (IMACM)

Preprint BUW-IMACM 12/28

Christof Kaufmann, Michael Günther, Daniel Klagges, Matthias Richwin, Sebastian Schöps, Jan ter Maten

Coupled Heat-Electromagnetic Simulation of Inductive Charging Stations for Electric Vehicles

November 2012

http://www.math.uni-wuppertal.de

Noname manuscript No.
(will be inserted by the editor)

Coupled Heat-Electromagnetic Simulation of Inductive Charging Stations for Electric Vehicles

Christof Kaufmann · Michael Günther · Daniel Klagges · Matthias Richwin · Sebastian Schöps · E. Jan W. ter Maten

Abstract Coupled electromagnetic-heat problems have been studied for induction or inductive heating, for dielectric heating, for testing of corrosion, for detection of cracks, for hardening of steel, and more recently for inductive charging of electric vehicles. In nearly all cases a simple co-simulation is made where the electromagnetics problem is solved in the frequency domain (and which thus is assumed to be linear) and the heat equation in the time domain. One exchanges data after each time step (or after some change in the heat profile). However, the coupled problem is non-linear in the heat variable.

In this paper we propose to split the time domain in windows in which we solve the electromagnetics problem in frequency domain. We strengthen the coupling by iterations, for which we prove convergence. By this we obtain a higher accuracy, which will allow for larger time steps and also for higher order time integration. This

This work is supported by the German BMBF in the context of the SOFA project (grant number 03MS648E). The fifth author is supported by the 'Excellence Initiative' of the German Federal and State Governments and the Graduate School of Computational Engineering at Technische Universität Darmstadt.

Christof Kaufmann, Michael Günther, E. Jan W. ter Maten
Bergische Universität Wuppertal, Fachbereich C, Lehrstuhl für Angewandte Mathematik/Numerische Analysis, Bendahler Straße 31, D-42285 Wuppertal, Germany
E-mail: {kaufmann,guenther,termaten}@math.uni-wuppertal.de

Daniel Klagges, Matthias Richwin
Leopold Kostal GmbH & Co. KG, An der Bellmerei 10, D-58513 Lüdenscheid, Germany
E-mail: {d.klagges,m.richwin}@kostal.de

Sebastian Schöps
Technische Universität Darmstadt, Graduate School of Computational Engineering, Dolivostraße 15, D-64293 Darmstadt, Germany
E-mail: schoeps@gsc.tu-darmstadt.de

E. Jan W. ter Maten
TU Eindhoven, Dept. Mathematics & Computer Science, CASA, PostBox 513, NL-5600 MB Eindhoven, The Netherlands
E-mail: E.J.W.ter.Maten@tue.nl

fully exploits the multirate behavior of the coupled system. An industrial example illustrates the analysis.

Keywords Inductive charging · Coupled simulation · Co-simulation · Electromagnetic · Heat · Modeling · Dynamic iteration

1 Introduction

In today's development processes, simulation is becoming more and more important. One predicts physical behavior precisely – even for multiphysics systems, where many effects influence each other. In that sense the first prototypes can be replaced by simulation. This is called *virtual prototyping* and speeds up time-to-market considerably.
In this paper simulation of electromagnetic problems coupled with heat problems is considered. Well known applications are induction heating [9, 12], dielectric heating [7], e.g. used for microwave ovens, steel hardening of gears [10] and detection of cracks or corrosion in ships. We focus on the design process of an *inductive charging* station for electric vehicles.
In inductive charging the electromagnetic (EM) field is of main importance. It induces eddy currents in massive conductors. At the power levels used for charging of electric vehicles, these losses cause a significant amount of heat. The heat diffuses and changes temperature and properties of the materials, and thus also the EM field. These effects have to be considered in a two-way coupling: One way is the generation of heat via eddy current losses resulting from the EM field. The other is the influence of the temperature dependent material parameters on the EM field.
In contrast to [8] we focus here on the comparison of the different co-simulation methodologies.

2 Modeling

A simple time-domain model consists of the magnetic vector potential equation (1) for the electromagnetic problem and the heat equation (2) to describe the heat diffusion. It can be stated as

$$\nabla \times (\mu^{-1} \nabla \times \mathbf{A}) + \varepsilon \frac{\partial^2 \mathbf{A}}{\partial t^2} + \sigma(T) \frac{\partial \mathbf{A}}{\partial t} = \mathbf{J}_{\mathrm{src}} \tag{1}$$

$$\rho\, c \frac{\partial T}{\partial t} = \nabla \cdot (\mathbf{k} \nabla T) + Q, \tag{2}$$

in which the heat source density Q comes from the power loss terms caused by the eddy current losses and the currents in the coil

$$Q(\mathbf{A}, T) := \sigma(T) \frac{\partial \mathbf{A}}{\partial t} \cdot \frac{\partial \mathbf{A}}{\partial t} - \mathbf{J}_{\mathrm{src}} \cdot \frac{\partial \mathbf{A}}{\partial t}. \tag{3}$$

In (1) $\mathbf{A}$ is the magnetic vector potential, $\mathbf{J}_{\mathrm{src}}$ is the source current density. The electric conductivity σ is material and temperature dependent. The other material parameters

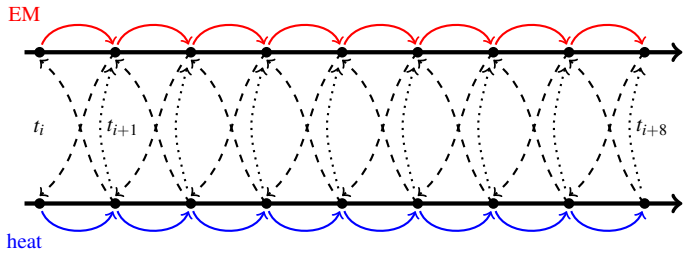

Fig. 1: Single rate co-simulation approach.

(the magnetic permeability μ and the permittivity ε) are considered here as constant in time and do not dependent on the temperature T, but vary in space. For the heat equation, ρ and c are the mass density and the specific heat density, respectively; $\mathbf{k}$ is the thermal conductivity. Both equations must be equipped with appropriate boundary conditions (BC). The heat equation requires an initial value (IV) at start time.

3 Co-Simulation

A simulation could be drawn out as one large system of equations, i.e. monolithic. Solving this system with classical time stepping methods would require to follow the demands of the fastest part of the system. In heat/electromagnetic problems this is usually the EM field. Here we assume a harmonic source current density, which determines the step size of the integrator. As first co-simulation scheme, we consider the one, that is closest to the monolithic approach: single rate co-simulation. Basically this is a Gauss-Seidel-type scheme, where each part uses the same time steps. The scheme is illustrated in Fig. 1. The single rate co-simulation approach is a simple and straight forward approach. Data of one part of the solution can be given directly into the next one. Alternatively, outer iterations can be used to increase the accuracy and stability. However, a lot of computational effort is spent in both subsystems due to the uniform time step, although the slow part does not need these steps. This observation is the base of the next scheme we consider.
The multirate co-simulation approach, illustrated in Fig. 2, makes use of the different time scales of the heat and EM equations. Since the source current density (and thus magnetic vector potential) is faster changing than the temperature, there are more time steps needed for the EM equation than for the heat equation. Clearly, here the advantage is the computational savings when solving the heat equation. On the other hand this approach is less straightforward than the single rate approach; one has to manage the more complex data transfer. A common way is the introduction of *synchronization time points* τ_i, as shown in the Fig. 2. This requires to align the time stepping schemes of all subsystems. Another way to find the data at the desired time point is interpolation. Finally, iteration is still possible in this multirate approach, similar to dynamic iteration approaches, e.g. [1]. However, the main part of the computational costs is the integration of the EM equation, which still has not changed in comparison to the single rate approach.

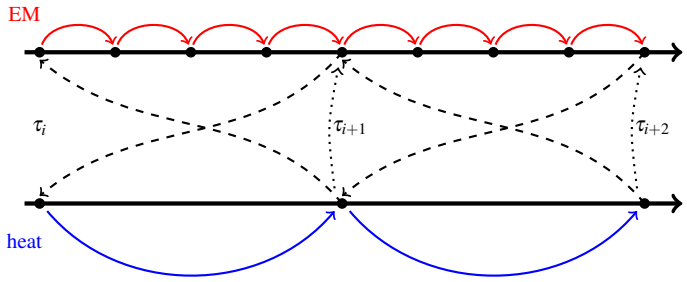

Fig. 2: Multirate co-simulation approach with synchronization time points τ_i.

3.1 Frequency-Transient Model

More elaborated modeling significantly reduces the high computational costs for solving the EM equation: for many applications it is accurate enough to average the power transferred within a time window $[\tau_i, \tau_{i+1}]$. Similarly, an averaged temperature, $\tilde{T}_i$, is used for the conductivity $\mathbf{M}_\sigma$ in the EM equation. For metals $\mathbf{M}_\sigma(T)$ is monotonically decreasing. The other material parameters (μ, ε) are assumed to be constant. That allows to solve the EM equation in the frequency domain and avoid the computation of the EM part in time domain. We further assume that $\mathbf{J}_{\text{src}} = \hat{\mathbf{J}}_{\text{src}}\, e^{j\omega t}$. Then the coupled model for a time harmonic source current density can be stated as

$$(j\,\omega\,\mathbf{M}_\sigma(\tilde{T}_i) - \omega^2\,\varepsilon)\hat{\mathbf{A}}_c + \nabla \times (\mu^{-1}\,\nabla \times \hat{\mathbf{A}}_c) = \hat{\mathbf{J}}_{\text{src}} \tag{4}$$

$$\rho\, c\, \frac{\partial T}{\partial t} = \nabla \cdot (\mathbf{k} \nabla T) + \tilde{Q}_i(\tilde{T}_i), \tag{5}$$

where

$$\tilde{Q}_i(\tilde{T}_i) = \mathbf{M}_\sigma(\tilde{T}_i)\, \frac{\omega^2}{2}\, \left\| \hat{\mathbf{A}}_c(\tilde{T}_i) \right\|_c^2 - \frac{\omega}{2}\, \mathrm{Im}\left(\overline{\hat{\mathbf{A}}_c(\tilde{T}_i)} \cdot \hat{\mathbf{J}}_{\text{src}} \right). \tag{6}$$

in which $\hat{\mathbf{A}}_c = \hat{\mathbf{A}}_c(\tilde{T}_i)$ and $\hat{\mathbf{J}}_{\text{src}}$ are the first Fourier coefficients of the magnetic vector potential $\mathbf{A}$ and the source current density $\mathbf{J}_{\text{src}}$, respectively. In (6) the norm is the complex norm; the overline indicates the complex conjugate. For further details of the derivation, see [8]. Remark that there is still the parametric coupling from the heat equation via the conductivity $\mathbf{M}_\sigma$ to the EM equation. Also the EM equation is still coupled to the heat equation via the source term $\tilde{Q}_i$. Hence, the coupling is still two-way. The EM equation (4) has become a purely algebraic equation whose solution depends on the temperature and, by this, implicitly on time. The scheme is illustrated in Fig. 3. By computing the EM equation in frequency domain only one linear system is solved for one time step of the heat equation. Especially for high frequencies this saves a huge amount of computational time in comparison to the classical approaches. Also, the data transfer is straightforward. This setup has been the basis for several coupled EM-heat problems [3,4,7,9], however typically without applying iterations.

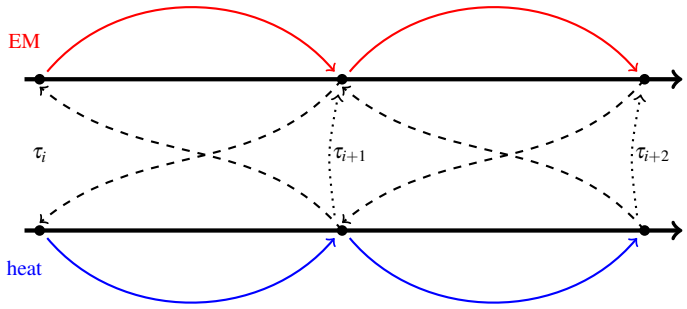

Fig. 3: Frequency-transient co-simulation approach.

When using an iterative scheme, convergence must be analyzed on beforehand. For the frequency-transient approach with an implicit Euler scheme for the time discretization of the heat equation, convergence can be proved [8]. This results in the following theorem:

Theorem 1 *We assume given BC and IV and differentiability for* $\mathbf{M}_\sigma$ *w.r.t. temperature* $\mathbf{t}$*. Then the iteration is convergent for h small enough with*

$$\left\| \mathbf{t}^{(l+1)} - \mathbf{t}^* \right\| \leq c(\omega) h \left\| \mathbf{t}^{(l)} - \mathbf{t}^* \right\|,$$

where $c(\omega)$ *is uniformly bounded on* $\omega \in [0,\infty)$*. Furthermore, for metals (*$\mathbf{M}'_\sigma < 0$*), we have* $c(\omega) = \mathcal{O}(\frac{1}{\omega^2})$ *for large* ω*.*

For metals this implies that there are no additional step size restrictions for $\omega \to \infty$. Then, for higher frequencies the step size can be larger. In fact this is in good agreement with the high frequency applications found in literature. However, we are also interested in rather moderate frequencies.

Proof: Here we summarize the steps of the proof; for details see [8]. We assume the same space discretization for both subproblems. For the discretization in space we propose Finite Element Method (FEM) with Lobatto Quadrature or the Finite Integration Technique (FIT), [11,4]. In the quadratic Q-term, the value of T only depends on the temperature in a local meshpoint. This simplifies the proof. For readability we drop the diacritic symbol $\hat{}$.
Let $\mathbf{a}$ and $\mathbf{t}$ denote the discretized magnetic vector potential and temperature, respectively. At time τ_n we assume $\mathbf{a},\mathbf{t}$ given. Then at $\tau_{n+1} = \tau_n + h$ we iteratively determine $\mathbf{t}^l \Rightarrow \mathbf{a}^{l+1} \Rightarrow \mathbf{t}^{l+1}$, etc. We assume that there is an exact solution without splitting error at τ_{n+1}: $\mathbf{a}^\star, \mathbf{t}^\star$. The *discretized EM equation* (4) becomes in FIT-like notation [11]

$$[j\omega \mathbf{M}_\sigma(\mathbf{t}^l) - \omega^2 \mathbf{M}_\varepsilon + \mathbf{C}^\top \mathbf{M}_\nu \mathbf{C}] \mathbf{a}^{l+1} = \mathbf{j}_{\mathrm{src}},$$

with diagonal matrices for conductivity, permittivity and reluctivity, $\mathbf{M}_\sigma$, $\mathbf{M}_\varepsilon$, $\mathbf{M}_\nu$, discrete curl operators $\mathbf{C}$, $\mathbf{C}^\top$ and source current $\mathbf{j}_{\mathrm{src}}$. This gives an error equation

$$[\mathbf{X}_{\varepsilon\nu} + j\omega \mathbf{M}^l_\sigma](\mathbf{a}^{l+1} - \mathbf{a}^\star) = -j\omega[\mathbf{M}^l_\sigma - \mathbf{M}^\star_\sigma]\,\mathbf{a}^\star,$$

where we define for convenience

$$\mathbf{X}_{\varepsilon\nu} := -\omega^2\mathbf{M}_\varepsilon + \mathbf{C}^\top\mathbf{M}_\nu\mathbf{C}, \qquad \mathbf{M}_\sigma^l := \mathbf{M}_\sigma(\mathbf{t}^l), \qquad \mathbf{M}_\sigma^\star := \mathbf{M}_\sigma(\mathbf{t}^\star).$$

Thus $\mathbf{a}^{l+1} = \mathbf{a}^\star + \mathbf{R}$, where

$$\mathbf{R} = -j\omega[\mathbf{X}_{\varepsilon\nu} + j\omega\mathbf{M}_\sigma^l]^{-1}[\mathbf{M}_\sigma^l - \mathbf{M}_\sigma^\star]\,\mathbf{a}^\star.$$

Hence

$$\|\mathbf{R}\| < \omega\|[\mathbf{X}_{\varepsilon\nu} + j\omega\mathbf{M}_\sigma^l]^{-1}\| \cdot \|\mathbf{M}_\sigma^l - \mathbf{M}_\sigma^\star\| \cdot \|\mathbf{a}^\star\|,$$

which asks for a uniform upper bound for the inverse operator and for Lipschitz continuity of $\mathbf{M}_\sigma$. Then the $\mathbf{a}^{l+1}$ are bounded.
The discretized version of the heat equation (5) is given in the following. For simplicity we assume time discretization by the implicit Euler scheme, we focus only on the quadratic term and disregard the other right-hand-side terms (rhs); $||.||$ is a vector of coordinate-wise norms

$$\begin{aligned}
[\mathbf{M}_{\rho,c} - h\tilde{\mathbf{S}}\mathbf{M}_k\tilde{\mathbf{S}}^\top(\mathbf{t}^{l+1} - \mathbf{t}^\star) &= \frac{1}{2}h\omega^2[\mathbf{M}_\sigma^{l+1}\|\mathbf{a}^{l+1}\|^2 - \mathbf{M}_\sigma^\star\|\mathbf{a}^\star\|^2] + \text{rhs} \\
&= \frac{1}{2}h\omega^2[\mathbf{M}_\sigma^{l+1}\|\mathbf{a}^\star + \mathbf{R}\|^2 - \mathbf{M}_\sigma^\star\|\mathbf{a}^\star\|^2] + \text{rhs} \\
&= \frac{1}{2}h\omega^2[\mathbf{M}_\sigma^{l+1} - \mathbf{M}_\sigma^\star]\,\|\mathbf{a}^\star + \mathbf{R}\|^2 + \mathscr{R} + \text{rhs} \\
\text{with } \mathscr{R} &= \frac{1}{2}h\omega^2\mathbf{M}_\sigma^\star[< \mathbf{a}^\star, \mathbf{R} > + < \mathbf{R}, \mathbf{a}^\star > + < \mathbf{R}, \mathbf{R} >]
\end{aligned}$$

with material matrices $\mathbf{M}_{\rho,c}$ and $\mathbf{M}_k$ and the divergence and gradient operators $\tilde{\mathbf{S}}$, $\tilde{\mathbf{S}}^\top$, respectively [4]. It follows equivalently

$$[\mathbf{M}_{\rho,c} - h\tilde{\mathbf{S}}\mathbf{M}_k\tilde{\mathbf{S}}^\top](\mathbf{t}^{l+1} - \mathbf{t}^\star) - \frac{1}{2}h\omega^2[\mathbf{M}_\sigma^{l+1} - \mathbf{M}_\sigma^\star]\,\|\mathbf{a}^\star + \mathbf{R}\|^2 = \mathscr{R}.$$

We can rewrite

$$[\mathbf{M}_\sigma^{l+1} - \mathbf{M}_\sigma^\star]\,\|\mathbf{a}^\star + \mathbf{R}\|^2 = \text{Diag}(\|\mathbf{a}^\star + \mathbf{R}\|^2)\,\text{Vec}(\mathbf{M}_\sigma^{l+1} - \mathbf{M}_\sigma^\star).$$

For the last term we can apply the mean value theorem coordinate-wise and thus get

$$\text{Vec}(\mathbf{M}_\sigma^{l+1} - \mathbf{M}_\sigma^\star) = \text{Diag}(\mathbf{M}'_{\sigma,k})(\mathbf{t}^{l+1} - \mathbf{t}^\star).$$

Hence, for $\mathbf{M}'_\sigma(T) < 0$ we have convergence for h small enough, but with good properties for varying ω. This completes the summary of the proof. □

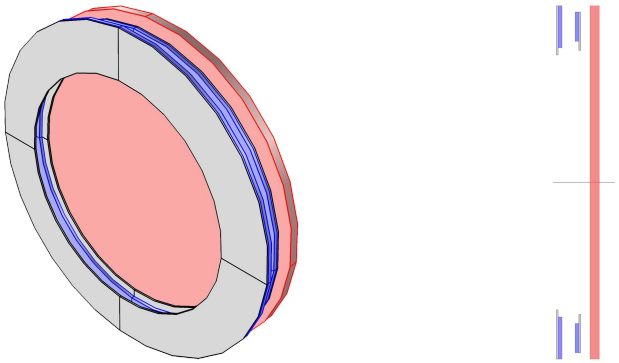

(a) 3d view on 2d-axisymmetric geometry.

(b) Cut view.

Fig. 4: Geometry of the simulated model. From left to right: ferrite (gray), primary coil (blue), air, secondary coil (blue), ferrite (gray), air, steel slice (red). The left coil represents the charging station and the right coil the coil behind the number plate in the car. (Comsol)

4 Generalization

For an extended approach by Driesen and Hameyer [6], where also the complex phasor is allowed to vary slowly, the proof can be extended. In this case the EM equation in frequency domain leads to a second order DAE after space discretization. Hence the error equation for the EM-equation needs to be integrated as well.
Another way of generalizing the frequency transient model is to include multifrequency excitation as needed, e.g., for non-smooth surfaces [10]. This is an easy way to allow approximations for other periodic waveforms of source currents. Other waveforms are important to approximate the current from power electronics, that control the primary coil. This gives way to a Harmonic Balance approach for the EM equation. It also allows for including a nonlinear permeability μ. Otherwise the model can only be used for a working point of the material curve.
A more general fully multirate time domain model, that exploits different time scales, can be derived by using the MPDAE approach by Brachtendorf [2]. By this, envelope simulation techniques from circuit simulation are applied to the coupled EM-heat problem.

5 Numerical Example

In this section results of a simulation for a model of an inductive charging system are shown. The simulation of a model with temperature independent conductivity, which results in a single way coupling, will be compared to the two-way coupling.
The frequency-transient model is applied to an inductive charging system for electric vehicles. The charging is done here through the number plate. The model consists of two copper coils with ferrite and air in between. The primary coil represents the

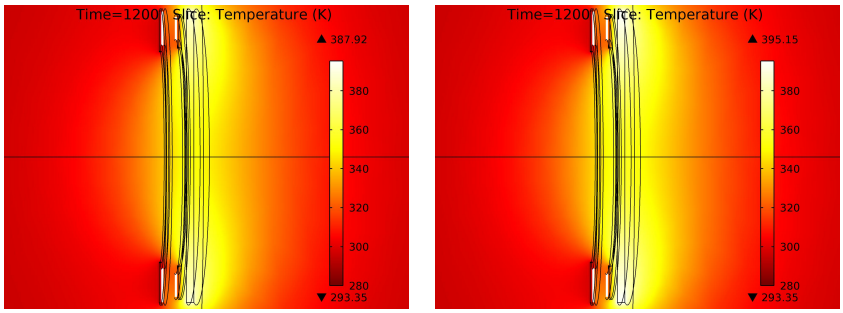

(a) Temperature independent conductivity. (b) Temperature dependent conductivity.

Fig. 5: Simulation of inductive charging system for e-cars after 20 min. The plot shows the temperature distribution. (Comsol)

charging station and the secondary coil the coil behind the number plate in the vehicle. To account for the challenges of a real world prototype, a steel bar with a constant permeability $\mu_r = 500$ is added behind the secondary coil. It models parts of the car body. The geometry is shown in Fig. 4.
The simulations are drawn out in Comsol [5] with appropriate settings to use the frequency-transient model as described in this paper. Simulation time is set to 20 min, the coils have 20 windings. The primary coil is excited by a current of 25 A at a (moderate) frequency of 10 kHz. The secondary has a zero current (no-load configuration). The conductivity σ in the independent case was chosen to be at room temperature (293.15 K), which is also the initial temperature.
The simulation with temperature independent conductivity shows a maximum temperature of 387.92 K, see Fig. 5a. The maximum temperature in case of an temperature dependent conductivity is 395.15 K, see Fig. 5b. The difference of about 7 K is due to the parameter coupling from the temperature to the EM equation via the conductivity.
Remark that for this simulation only 17 time steps were needed to compute the results. When we compare that to simulating this problem with a monolithic model and assume 10 time steps per period of the source current, 120 million time steps would be necessary for simulation. This clearly shows the efficiency of simulation of the frequency-transient model compared to approaches, where the EM equation is solved in time domain.

6 Conclusions

A frequency-transient model tailored for coupled heat-electromagnetic problems was described. An efficient multirate co-simulation approach was proposed for solving it it. For this algorithm a convergence theorem for an iterative approach was proved for all frequencies. For metals and higher frequencies the speed of convergence increases. The numerical example confirms this result. The theorem also applies to approaches by Driesen and Hameyer [6] and implementations in Comsol [5]. In particular it

applies to many cosimulation approaches for high frequency applications [3,4,7,9, 10,12]. From the analysis (see [8]) an optimal step size can be derived.

References

1. Bartel, A., Brunk, M., Günther, M., Schöps, S.: Dynamic iteration for coupled problems of electric circuits and distributed devices. SIAM J Sci Comput (2012). Accepted
2. Brachtendorf, H.G., Welsch, G., Laur, R., Bunse-Gerstner, A.: Numerical steady state analysis of electronic circuits driven by multi-tone signals. Electrical Engineering (Archiv fur Elektrotechnik) **79**, 103–112 (1996). 10.1007/BF01232919
3. Chen, H., Tang, J., Liu, F.: Coupled simulation of an electromagnetic heating process using the finite difference time domain method. J Microw Power Electromagn Energy **41**(3), 50–68 (2007)
4. Clemens, M., Gjonaj, E., Pinder, P., Weiland, T.: Numerical simulation of coupled transient thermal and electromagnetic fields with the finite integration method. IEEE Trans. Magn. **36**(4), 1448–1452 (2001). DOI 10.1109/20.877711
5. COMSOL Multiphysics: Command reference (2007). URL `www.comsol.com`
6. Driesen, J., Hameyer, K.: The simulation of magnetic problems with combined fast and slow dynamics using a transient time-harmonic method. Eur Phys J Appl Phys **14**, 165–169 (2001). DOI 10.1051/epjap:2001155
7. Janssen, H., ter Maten, E., van Houwelingen, D.: Simulation of coupled electromagnetic and heat dissipation problems. IEEE Trans Magn **30**(5), 3331–3334 (1994). DOI 10.1109/20.312651
8. Kaufmann, C., Günther, M., Klagges, D., Richwin, M., Schöps, S., ter Maten, J.: Efficient simulation of frequency-transient mixed co-simulation of coupled heat-electromagnetic problems (2012). Submitted for Proceedings SCEE 2012.
9. ter Maten, E., Melissen, J.: Simulation of inductive heating. IEEE Trans Magn **28**(2), 1287–1290 (1992). DOI 10.1109/20.123925
10. Rudnev, V.: Induction hardening of gears and critical components. Gear Technology pp. 58–63 (Sept/Oct) and 47–53 (Nov/Dec) (2008). Part I and II.
11. Weiland, T.: Time domain electromagnetic field computation with finite difference methods **9**(4), 295–319 (1996). DOI 10.1002/(SICI)1099-1204(199607)9:4<295::AID-JNM240>3.0.CO;2-8
12. Will, J.: An optimal control problem in electromagnetic induction heating. Master's thesis, Chemnitz University of Technology, Department of Mathematics, Germany (2010)